

Impact Testing of a Thermosetting Polymer (Allyl Diglycol Carbonate—CR39)[®]

V. R. HOWES, J. M. GOLDSMID, R. K. SILK, and A. V. WERE,
Department of Applied Physics, University of New South Wales, Australia

Synopsis

Allyl diglycol carbonate (CR39)[®] is a thermosetting polymer of interest both as an ophthalmic material and as a material intermediate between brittle and ductile solids. The response to impact in the crack-threshold range has been studied and compared to that of glass. The energy absorbed upon impact, the plastic deformation, and the crack resistance are all found to be greater for CR39, and the relationships between these factors are discussed. The developments of impact response for CR39 with increasing temperature and increasing impact energy beyond the crack-threshold range have also been studied.

INTRODUCTION

With the development of comparatively hard and scratch-resistant polymeric crosslinked resins, plastics have established a competition with glass for use as ophthalmic lenses as well as safety visors and goggles. The advantages are that the plastic lenses are lighter and more resistant to fracture.¹ The resistance to cracking of such polymeric resins is rate-dependent; often, cracking can be easily induced by dynamic impact in contrast to the absence of cracking under quasistatic indentation at room temperature. As the service life of any component (dependent upon mechanical strength, static or dynamic fatigue resistance, or chemically enhanced failure, e.g., solvent cracking) is likely to be strongly affected by the presence of surface flaws or cracks,² the resistance to cracking under all surface loading conditions is important, whether the conditions relate to abrasion or particle impact.

These relatively hard crosslinked polymer resins have an additional interest with respect to fracture phenomena. They are semibrittle, as indicated above by the rate dependency of their cracking. Thus, they form a phenomenological link between the typically brittle materials such as glass and the effectively nonbrittle materials such as the polycarbonates. Upon impact, the crosslinked polymers show both the cracking characteristic of the former and the macroplastic deformation characteristic of the latter.

Impact fracture testing of polymers has been extensive and is well described in a recent review by Reed.³ However, the emphasis has been on complete failure rather than on the initiation of cracks which may ultimately lead to failure. In this study we concentrate on crack initiation resistance of ophthalmic materials, using a falling-weight type of impact test in which a spherically tipped impactor is dropped onto the specimen. The materials selected for this initial study were the Columbia Resin of allyl diglycol carbonate (CR39)[®] which is a thermosetting crosslinked polymer and, for comparison purposes, Pilkington float glass. Impact tests were also carried out on CR39 at its maximum continuous service temperature of 100°C.

EXPERIMENTAL

The apparatus used was similar to that in the standard ASTM-D1709-75,⁴ in which a spherically tipped metal dart of variable mass is released from a fixed height to fall freely onto a peripherially supported circular disc specimen. However, by allowing for variation of drop height, the dependency of resistance to cracking upon rate of impact could be studied independent of the impact energy. Also, since surface crack initiation was of primary concern, the specimens were fully supported at the back surface.

The impactor head was a 1-mm-diameter tungsten carbide sphere, mounted on a steel support, as shown in Figure 1(a). This support could be screwed firmly onto different lengths of solid cylinders of steel [Fig. 1(a)], so that the impacting mass (m) could be varied (between 2.5 g and 16 g). By dropping the impactor

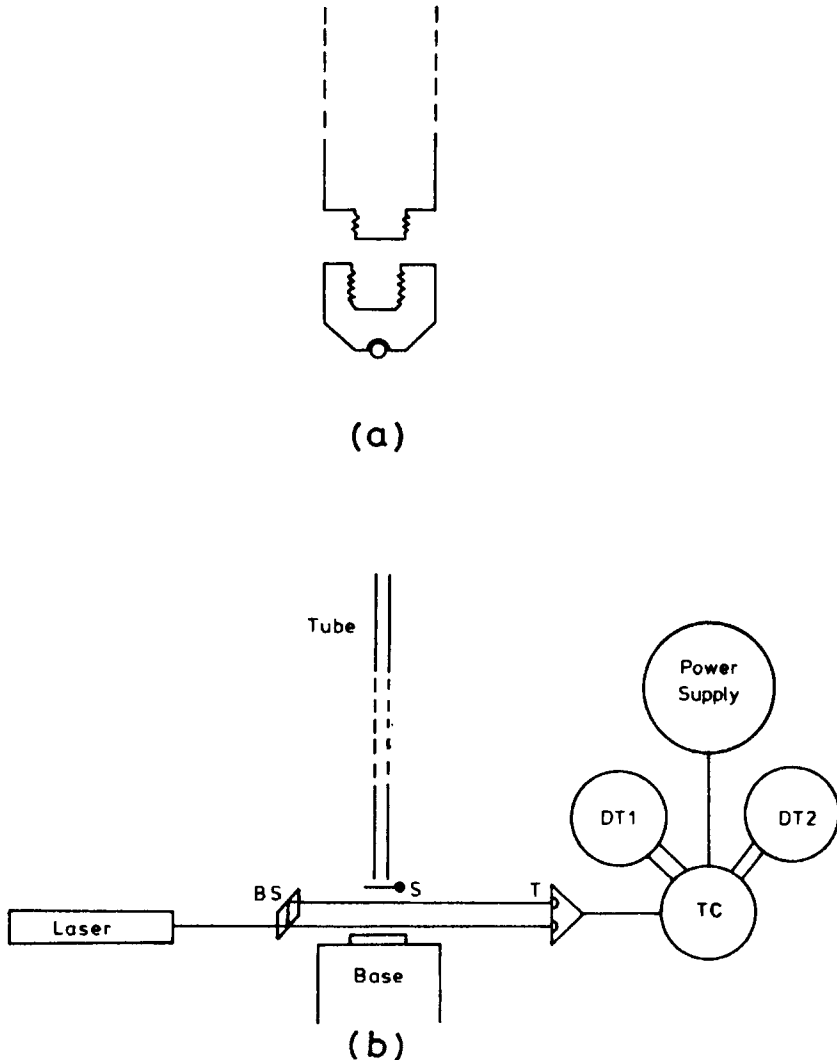


Fig. 1. (a) The impactor comprising a 1-mm-diam tungsten carbide sphere mounted on a steel support that can be screwed onto different lengths of steel rod. (b) The experimental arrangement for impact testing. (BS) beam splitter; (T) phototransistors; (TC) trigger circuit; (DT) digital timers; (S) shutter (prevents rebound).

from different heights, the velocity of impact could be varied (between $0.75 \text{ m}\cdot\text{s}^{-1}$ and $5 \text{ m}\cdot\text{s}^{-1}$). The velocity of impact (v_i) was accurately determined by measuring the time between the intersections of the falling impactor with two parallel light beams separated by 1 cm, immediately above the specimen. The arrangement, shown in Fig. 1(b), was also able to measure the rebound velocity of the impactor (v_b). The impactor was held and released electromagnetically, and the trigger circuit, in addition to switching the digital timers on and off, also activated a shutter so that secondary impacts were prevented.

With this apparatus, independent variation of mass and drop height gave independent selection of energy and velocity, so that, for example, tests could be carried out at different impact velocities but with the same impact energy. The coefficient of restitution could be measured ($R = v_b/v_i$) or the ratio of energy loss to impact energy ($\Delta E/E_i = (\frac{1}{2}mv_i^2 - \frac{1}{2}mv_b^2)/\frac{1}{2}mv_i^2$). Observation by microscope after each test established whether or not a ring-crack had been formed at the surface. Even at fixed values of E_i and v_i , sometimes ring cracks were formed upon impact and sometimes not. Repetitive tests allowed a probability P to be calculated (P being the ratio of the number of tests giving ring cracks to the total number of exactly similar tests). From the variation of P and E_i an estimate of the resistance to cracking was obtained by the probit statistical method,³ in which the critical impact energy is defined as that which gives $P = 0.5$. This critical impact energy is referred to here as E_{50} (this is to be distinguished from the more familiar F_{50} value referring to 50% complete failure of specimens).

The specimens were 50-mm-diameter discs, 2 mm thick. The CR39 samples were plano lenses with optical quality surface finish; the glass had a "float" quality finish. The base that supported the unclamped specimens was the polished flat end of a solid brass cylinder, 10 cm in diameter and 40 cm long, standing on a concrete floor. For tests at elevated temperatures, the specimen, support, and end of the dropping tube were surrounded by a vertical split-cylinder furnace.

RESULTS

The relationship for CR39 between dissipated energy (ΔE) and impact energy (E_i) at room temperature (20°C) is shown in Figure 2, for 21 experiments carried out at six different impact velocities. Each experimental point is the mean for 20 repeated impact tests; the only difference between these tests was whether or not a ring crack formed upon impact. Within the limits of measurement of these experiments, the value of $\Delta E/E_i$ was found to be independent of the incidence of cracking, of E_i , and of v_i in the range $1\text{--}5 \text{ m}\cdot\text{s}^{-1}$. The mean value of $\Delta E/E_i$ for all the experiments indicated in Figure 2 was calculated as 0.60 ± 0.02 (standard deviation). The results of similar experiments on float glass are also shown in Figure 2. Again, independence of $\Delta E/E_i$ with respect to E_i , v_i , and cracking was found, but for float glass the calculated value of $\Delta E/E_i$ was equal to 0.47 ± 0.11 .

Figure 3 shows the probability of cracking (plotted with a normal probability scale) against E_i for CR39 and float glass. To obtain a measure of the resistance to cracking, the value of E_i for $P = 0.5$ (E_{50}) was estimated by interpolations from this graph. The results showed no measurable dependence of E_{50} on v_i , for the range $1\text{--}5 \text{ m}\cdot\text{s}^{-1}$, for either material. The value of E_{50} for CR39 can be seen to be $12 \pm 2 \text{ mJ}$. The experiments on float glass gave E_{50} as $3 \pm 2 \text{ mJ}$.

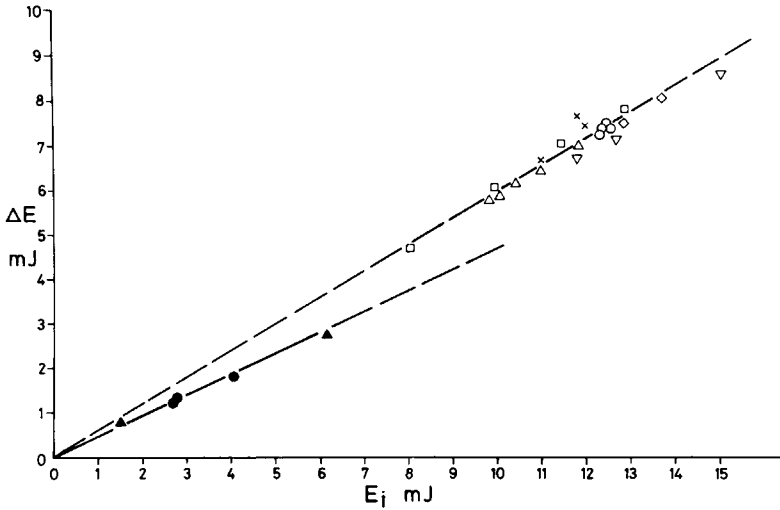


Fig. 2. Graph of energy loss of impactor (ΔE) against impact energy (E_i) for CR39 and for glass. CR39: (Δ) 1.1 m·s⁻¹; (∇) 1.2 m·s⁻¹; (\diamond) 2.3 m·s⁻¹; (\square) 2.5 m·s⁻¹; (\times) 3.4 m·s⁻¹; (\circ) 4.3 m·s⁻¹. Glass: (\bullet) 0.75 m·s⁻¹; (\blacktriangle) 1.0 m·s⁻¹.

The appearance of the specimen surfaces after impact was observed by optical microscope. A typical ring crack produced on CR39 in these tests is shown in Figure 4(a). For the impact energies involved in establishing E_{50} , the cracks sometimes formed complete rings, sometimes short arcs. Microscopic examination showed little sign of deformation on CR39 after impact, apart from the

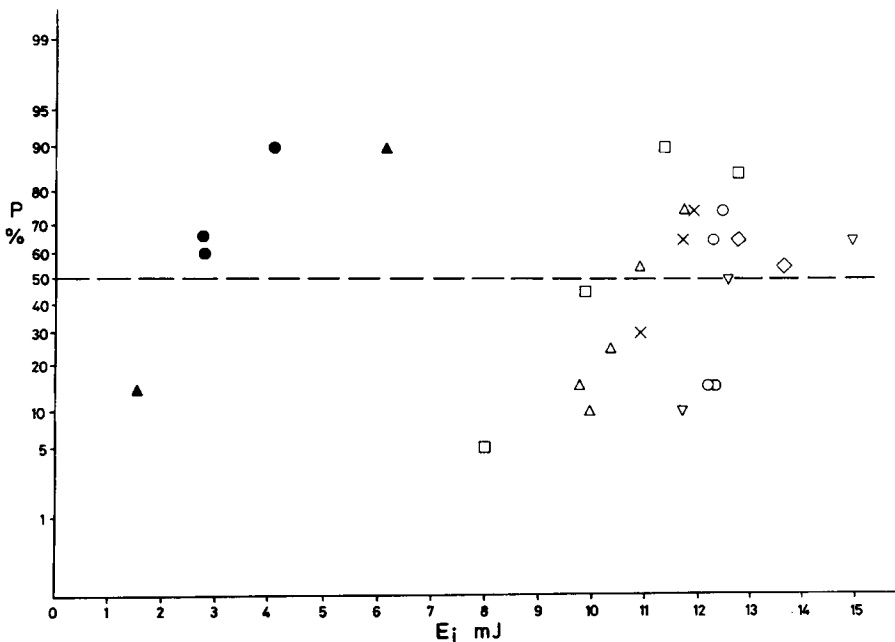


Fig. 3. Graph of probability of cracking (P) against impact energy (E_i) for CR39 and for glass. CR39: (Δ) 1.1 m·s⁻¹; (∇) 1.2 m·s⁻¹; (\diamond) 2.3 m·s⁻¹; (\square) 2.5 m·s⁻¹; (\times) 3.4 m·s⁻¹; (\circ) 4.3 m·s⁻¹. Glass: (\bullet) 0.75 m·s⁻¹; (\blacktriangle) 1.0 m·s⁻¹.

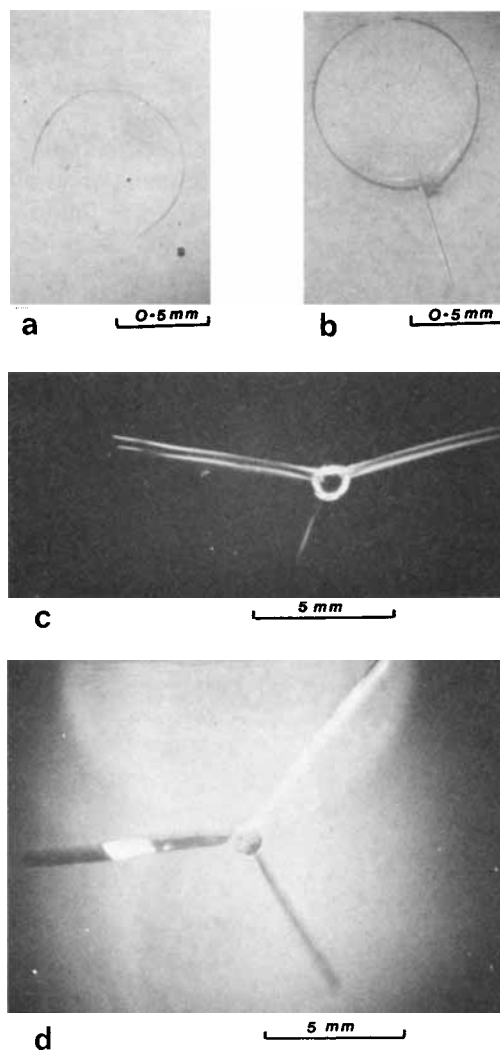


Fig. 4. Impact cracking on CR39 at room temperature: (a) at crack threshold impact energy (E_{50}); (b) at impact energy equal to $3E_{50}$; (c) at impact energy equal to $7E_{50}$, specimen tilted at 45° to the camera; (d) at impact energy equal to $14E_{50}$.

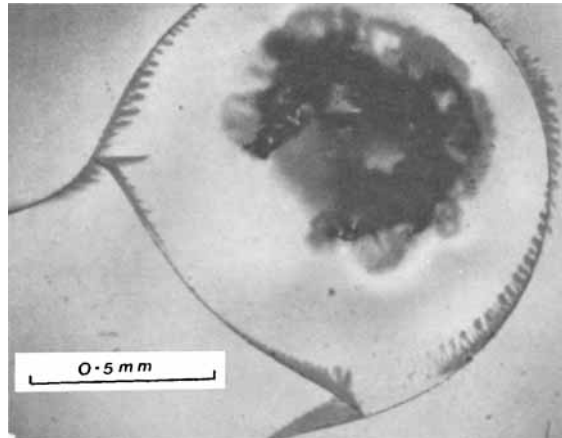
ring cracks. However, unlike glass, smooth depressions were observed macroscopically.

In order to study the development of impact damage on CR39 beyond the crack-threshold region described above, a series of tests was done at higher impact energies. The impact velocity was kept constant at $4 \text{ m}\cdot\text{s}^{-1}$, close to the maximum obtainable. The qualitative results, at impact energies expressed in multiples of E_{50} , were as follows. For $E_i = 3 E_{50}$, in addition to ring cracks, shallow radial cracks were formed in the top surface of the specimen at the ring crack, as shown in Figure 4(b). For $E_i = 7 E_{50}$, Figure 4(c) shows a typical impact site (specimen tilted at 45° to camera), where the shallow radial cracks have formed at both the top and bottom surfaces of the specimen, immediately opposite each other but apparently with uncracked material in the body of the

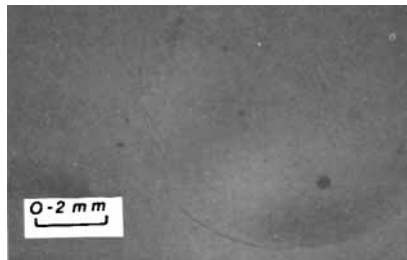
specimen between the two surface cracks. For $E_i = 14 E_{50}$, approximately half of the specimens tested fractured completely. Where complete separation had not occurred, the radial cracks were observed to be continuous through the thickness of the specimen, as shown in Figure 4(d).

The effect of higher temperatures upon impact damage of CR39 was studied by carrying out similar impact tests on specimens maintained at 100°C (the maximum continuous-service temperature). It was found that the amount of permanent plastic deformation increased and that cracks occurred only at much higher impact energies. For maximum experimentally attainable impact velocity of $4.3 \text{ m}\cdot\text{s}^{-1}$, a series of experiments, following the procedure used at room temperature, gave $E_{50} = 45 \pm 5 \text{ mJ}$. However, at the upper end of this impact energy range and beyond, an entirely new form of cracking was observed—in the center of the ring cracks, as can be seen in Figure 5(a). Not seen at all below approximately 50-mJ impact energy, this type of central cracking was predominant at approximately 60-mJ impact energy, then often being seen without an accompanying ring crack.

Finally, the balance between the effects of impact rate and temperature upon fracture was demonstrated by indentation at low temperatures. Although under quasistatic loading with a spherical indenter, ring cracks were never observed on CR39 at room temperature or at approximately -50°C . Figure 5(b) shows the peripheral cracks that were produced upon indenting a sample of CR39 cooled with liquid nitrogen.



(a)



(b)

Fig. 5. (a) Impact cracking on CR39 at 100°C . (b) Peripheral cracking observed after quasistatic loading of CR39 cooled with liquid nitrogen.

DISCUSSION

The deformation of a specimen undergoing impact may be elastic, plastic, viscoelastic with subsequent recovery, brittle with cracking, possibly followed by fragmentation or crushing. The total deformation will be some combination of these types of deformation. The energy redistribution upon impact must be shared by the impactor, the specimen, and the support. For a complete energy analysis of impact, the effects of stress wave transmission, internal friction, vibrations, and interfacial friction (between impactor and specimen and between specimen and support) must also be considered. If the impact rate is high enough, the deformational changes tend to be adiabatic, with consequent temperature rises leading to softening if not melting (even ceramics can melt under impact⁵). Such temperature changes must inevitably modify the deformation characteristics.

In this initial study of impact of ophthalmic materials, much of this daunting complexity was sidestepped by restricting the results to comparison of two materials and looking at qualitative trends. Nevertheless, the low value of the coefficient of restitution obtained for glass ($R = 0.73$ for $\Delta E/E_i = 0.47$) compared to $R \approx 0.93$ obtained for glass spheres dropped on glass by Kirchner and Gruver⁶ is most likely explained by the larger energy absorption in the more complex impactor used here [see Fig. 1(a)].

The significantly greater value of fractional energy loss ($\Delta E/E_i$) for CR39 than for glass (0.60 compared with 0.47) is due to the greater absorption of energy in the impacted CR39 specimens associated with an enhanced macroplastic deformation (for the glass this was zero). The independence of the $\Delta E/E_i$ values upon the incidence of cracking is an indication of the relatively insignificant amount of energy associated with the formation of the crack compared with other energy expenditures. This independence was observed for glass as well as CR39 and is in agreement with the findings of Tsai and Kolsky⁷ and Kirchner and Gruver.⁶ The fact that no variation of $\Delta E/E_i$ or E_{50} with impact velocity (v_i) was detected at constant E_i is probably due to the limited range of values obtainable with the apparatus used ($1-5 \text{ m}\cdot\text{s}^{-1}$); it is hoped to extend this range in future work. The decrease in R (and thus the increase in $\Delta E/E_i$) with v_i observed by the above authors was for impacting spheres of constant mass so that E_i was considerably increased as v_i was increased.

The resistance to cracking, or impact strength, as measured by the value of E_{50} , was found to be approximately four times greater for CR39 than for glass at room temperature (12 mJ compared to 3 mJ for the test used). For CR39 the E_{50} value at 100°C was almost four times greater than at room temperature (45 mJ compared to 12 mJ for the test used). This marked increase of impact strength with temperature is in agreement with the results of impact testing of other polymeric materials by Vincent.⁸ Both of the above increases in E_{50} values are associated with a marked increase in plastic deformation of the specimen upon impact (from glass to CR39 and from CR39 at room temperature to CR39 at 100°C). Thus it appears that, as plastic deformation upon impact increases, the resistance to cracking of the material increases, i.e., the less likely it is that the surface stresses will build up to the critical value for ring-crack initiation. Wolstenholme et al.⁹ found a similar increase in impact strength, or breaking energy, with amount of plastic yielding associated with cracking upon impact, but that was for thermoplastic polymers. For the more brittle thermosetting

polymer resins, the brittleness, or extent to which plastic deformation occurs under high loading, depends upon the amount of crosslinking that has been induced by the curing of the polymers, as well as upon the strain rate and temperature. In a recent review of the fracture of these materials, Young¹⁰ states that plastic deformation undoubtedly takes place at the crack tip during fracture. Of course, silicate glass at room temperature represents the extreme of no plastic yielding for the impact range considered or for controlled fracture, but the above considerations do make high-temperature impact strength testing of glass an attractive future possible extension of the present work.

The considerable increase in the E_{50} value of CR39 at 100°C compared with room temperature may well indicate a brittle/ductile transition at a somewhat higher temperature; however, the central cracking observed after impact at 100°C [Fig. 5(a)] certainly indicates a mode of cracking transition which is sensitive to impact rate and temperature. The complex appearance of this cracking, which does not seem to conform to any of the other crack systems associated with the impact of materials (cone, radial, median, or lateral cracking, crazing or stress whitening), suggests that it might play a greater energy-absorbing role than the simple ring crack obtained at lower temperatures. The sensitivity of cracking of CR39 to impact rate and temperature is again shown up by the cracking produced [Fig. 5(b)] even under quasistatic loading when the temperature is low enough.

Several investigators have observed the development of a variety of additional crack systems as the impact energy exceeds that which initiates ring cracks on brittle materials (see, for example, Ref. 7). In the present experiments for CR39 at room temperature, the first development at higher impact energies of shallow radial cracks in addition to the peripheral ring cracks [see Fig. 4(b)] is not dissimilar to the observations of Kirchner and Gruver on glass at high impact velocities and high temperatures.⁶ However, the subsequent development of twin shallow radial cracks on the front and back surfaces of the 2-mm-thick specimens for higher impact energies, and the apparent coalescence of these twin cracks at still higher impact energies [see Figs. 4(c) and 4(d)], show a surprisingly controlled evolution of radial crack development with increasing impact energy, at constant impact velocity.

CONCLUSIONS

1. In the crack-threshold range of impact, there is greater energy absorption for CR39 than for glass and greater plastic deformation.

2. The greater crack resistance of CR39 compared to glass, and the greater crack resistance of CR39 at 100°C compared to that at room temperature, are related to the observed greater plastic deformation during impact in each case.

3. For impact of CR39, there is a threshold crack mode transition as the temperature is increased, from ring cracking to central cracking at the impact site.

4. As the impact energy increases beyond the ring-crack threshold range of CR39 at room temperature, there is a development of radial cracks, shallow at first, then growing on both surfaces and finally extending through the depth of the sheet specimens prior to complete failure.

The authors wish to thank Professor B. R. Lawn for valuable comments. The CR39 samples were supplied by Protector Safety Products Pty., Ltd., Australia, and the float glass was supplied by Pilkington A.C.I. Ltd., Australia.

References

1. A. W. Newton, *J. Inst. Eng. Aust.*, **39**, 163 (1967).
2. B. R. Lawn and T. R. Wilshaw, *Fracture of Brittle Solids*, Cambridge University Press, Cambridge, 1975.
3. P. E. Reed, *Developments in Polymer Fracture—1*, E. H. Andrews, Ed., Appl. Sci. Publ., London, 1979, Chap. 4, p. 121.
4. ASTM-D 1709-75, "Test for Impact Resistance of Polyethylene Film by the Free-Falling Dart Technique."
5. B. R. Lawn, B. J. Hockey, and S. M. Wiederhorn, *J. Am. Ceram. Soc.*, **63**, 356 (1980).
6. H. P. Kirchner and R. M. Gruver, *Fracture Mechanics of Ceramics, Vol. 3*, R. C. Bradt, D. H. P. Hasselman, and F. F. Lange, Eds., Plenum, New York, 1978, p. 365.
7. Y. M. Tsai and H. Kolsky, *J. Mech. Phys. Solids*, **15**, 263 (1967).
8. P. I. Vincent, *Impact Tests and Service Performance of Plastics*, Plastics Institute, London, 1971.
9. W. E. Wolstenholme, S. E. Pregun, and C. F. Stark, *J. Appl. Polym. Sci.*, **8**, 119 (1964).
10. R. J. Young, *Developments in Polymer Fracture—1*, E. H. Andrews, Ed., Appl. Sci. Publ., London, 1979, Chap. 6, p. 183.

Received February 27, 1981

Accepted April 13, 1981